CHAPTER 22

TRANSFER LINE OPTICS AND LAYOUT

22.1 INTRODUCTION

This chapter describes the layout and optics design of TI 2 and TI 8 [1], the trajectory correction scheme [2] and the required performance. Careful control of the trajectory and the preservation of the very small emittance during transfer and injection are of key importance, because of the very limited mechanical aperture of the line magnets [3], the high intensity and energy in the beam, the limited numbers of correctors and pick-ups and the tight tolerances on the beam parameters at injection into the LHC [4].

Details of the magnets, powering, vacuum civil engineering and other services (water, ventilation and transport) are covered elsewhere in the LHC design report.

22.1.1 Design Goals

The transfer lines must allow the beams to be injected onto the LHC orbit with high precision and reproducibility [5] while ensuring an adequate optical match and remaining sufficiently flexible to accommodate any future machine optics changes. The machine protection elements in the lines should prevent the transfer of beams which could cause damage to the LHC, either by generating interlocks, or by passive protection. The main performance specifications for the lines are given in Tab. 22.1.

Table 22.1: Main performance specification for the transfer lines (tolerance values).

Parameter	**Unit**	**Value**
Beam emittance from SPS (1 σ normalised)	μm	3.5
Beam energy	GeV	450
Maximum beam intensity	p+	$4.9 \times 10^{+13}$
Beam energy spread (1 σ)	Δp/p	0.0015
Energy acceptance	Δp/p	±0.003
Injection precision in LHC	σ	±1.5
Tuning range for SPS optical parameters at extraction point (β, α)	%	±20
Tuning range for LHC optical parameters at injection point (β, α)	%	±20
Transverse emittance growth from all mismatch effects	$\varepsilon/\varepsilon_0$	1.05
Transverse oscillation amplitude transmitted into the LHC for failure cases	σ	±7.5
Aperture	σ	±6.0

22.2 GEOMETRICAL LAYOUT

The geometrical layout of the lines is dictated by:

- The choice of SPS points 4 and 6 for the location of the fast extraction systems
- The choice of LHC points 8 and 2 for the corresponding injection systems
- By the relative geometries of the two machines
- The magnetic rigidity of the beam extracted from the SPS
- The strength of the main bending dipoles in the lines.

For LHC Ring 1, the beam is extracted from SPS LSS6 [6] and transferred to LHC Point 2 by the existing TT60 transfer line and TI 2. For Ring 2 the beam is extracted in SPS LSS4 [7] and transferred via TT40 and TI 8. The total horizontal and vertical deflections and offsets of the combined TT60-TI 2 and TT40-TI 8 lines are given in Tab. 22.2. The horizontal and vertical sections of the lines are shown in Fig. 22.1

The SPS is aligned in the plane normal to the local gravity vector at the centre of the SPS accelerator. The plane of the SPS is therefore tilted with respect to the CERN Coordinate system (CCS) by 0.24 mrad. Note

that this angle is also the maximum of the slope ϕ to be found in the SPS ring. For geological reasons associated with the civil engineering of the tunnel, the plane of the LHC machine was built at a fairly large angle of 1.4% (14 mrad) to the CCS. The geometrical matching of the lines must therefore respect the alignment differences between the two machines, as summarised in Tab. 22.2. In this table the extraction point of the SPS is defined as the exit plane of the quadrupole QDA4(6)19 coil window and that the injection point of the LHC is defined as the entrance of the first injection septum MSI. The XYZ coordinates in Tab.22.2 are given in the CERN coordinate system, where Y represents the altitude.

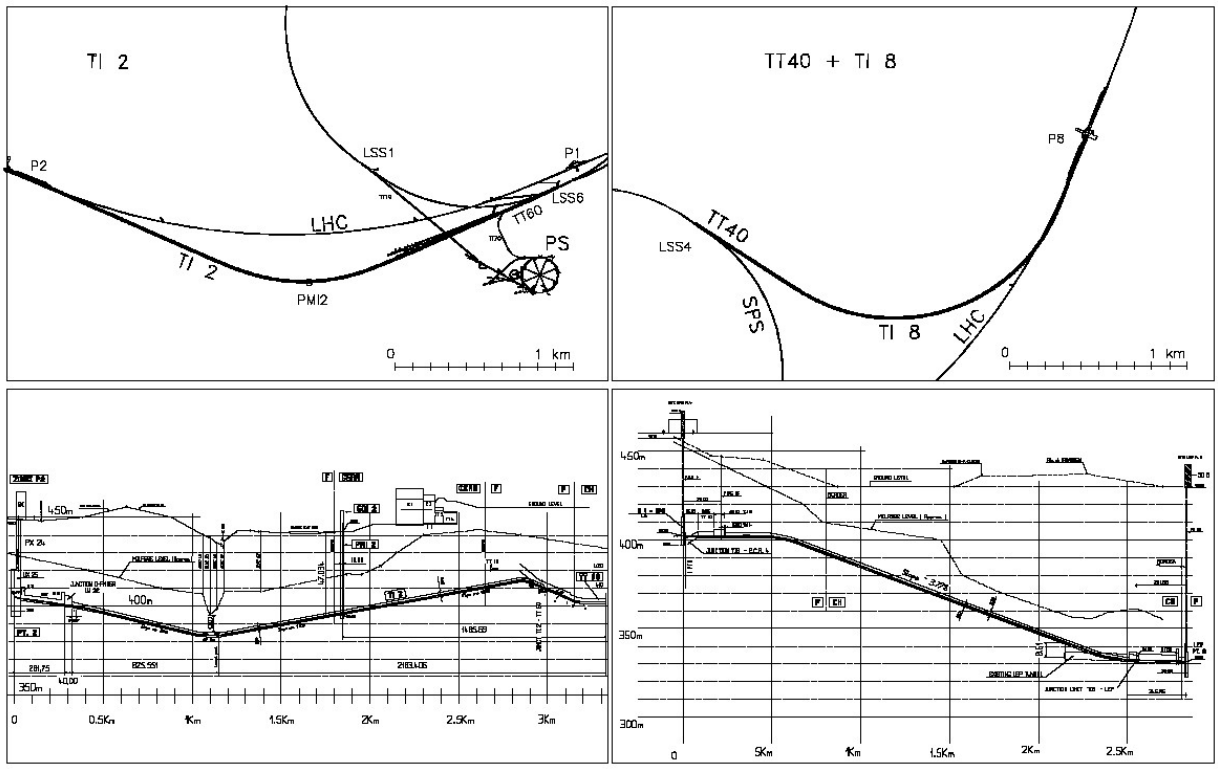

Figure 22.1: Horizontal and vertical sections of TI 2 and TI 8.

Table 22.2: Main geometrical parameters of TI 2 and TI 8.

Parameter	**Unit**	**TI 2**	**TI 8**
Length	m	3116.732	2627.501
Vertical height difference	m	1.124	70.875
Horizontal bending angle	degree	48.22	103.04
Vertical bending angle	degree	6.5	4.3
Maximum vertical slope	degree	4.3	3.8
SPS extraction point location: X	m	-2083.528	-2314.717
Y	m	2402.179	2401.752
Z	m	2586.131	4456.102
LHC injection point location: X	m	817.045	-4391.382
Y	m	2401.056	2330.877
Z	m	2615.609	4807.174

22.3 OPTICS

Both lines use a FODO lattice with 90° phase advance per cell and a half-cell length of 30.3 m. The structure is similar to the SPS with each half-cell containing four dipoles, as shown in Fig. 22.2. Short straight sections with space for instrumentation and dipole corrector magnets follow each quadrupole, as illustrated in Fig. 22.3. The main optical parameters and requirements are summarised in Tab. 22.3.

The main horizontal arc in TI 2 has been designed as an achromat. Space reasons dictated a different solution for TI 8. Beam optics calculations to second order show negligible effects which do not require higher-order corrections. The optics functions for TI 2 and TI 8 are shown in Fig. 22.4 and 22.5 respectively

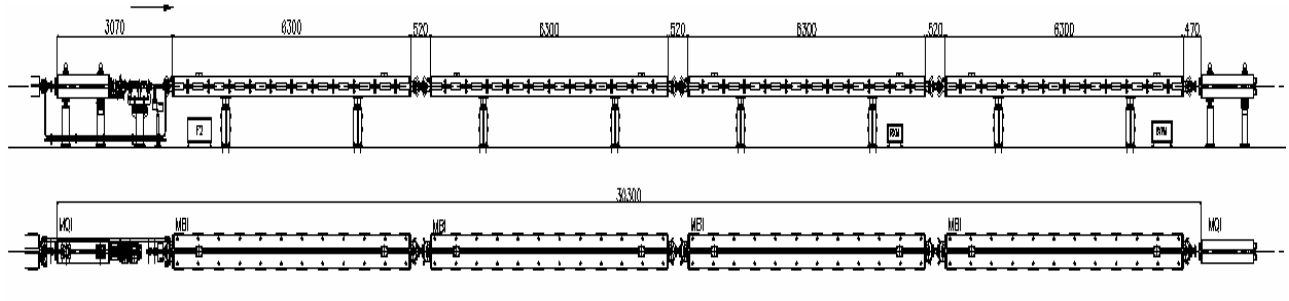

Figure 22.2: Half-cell layout (MBI version).

Table 22.3: Summary of main optics parameters for the transfer lines.

Parameter	**Unit**	**TI 2**	**TI 8**
β_x max	m	308.5	240.8
β_y max	m	289.5	274.6
β_x max (arc section)	m	101.2	101.2
β_y max (arc section)	m	101.1	101.1
$\|D_x\|$ max	m	3.82	3.88
$\|D_y\|$ max	m	3.97	1.34
D_x rms	m	1.42	1.78
D_y rms	m	0.55	0.20
μ_x total	2π	12.07	10.54
μ_y total	2π	12.24	10.32
Half-cell length	m	30.3	30.3
Number of half-cells		95	85

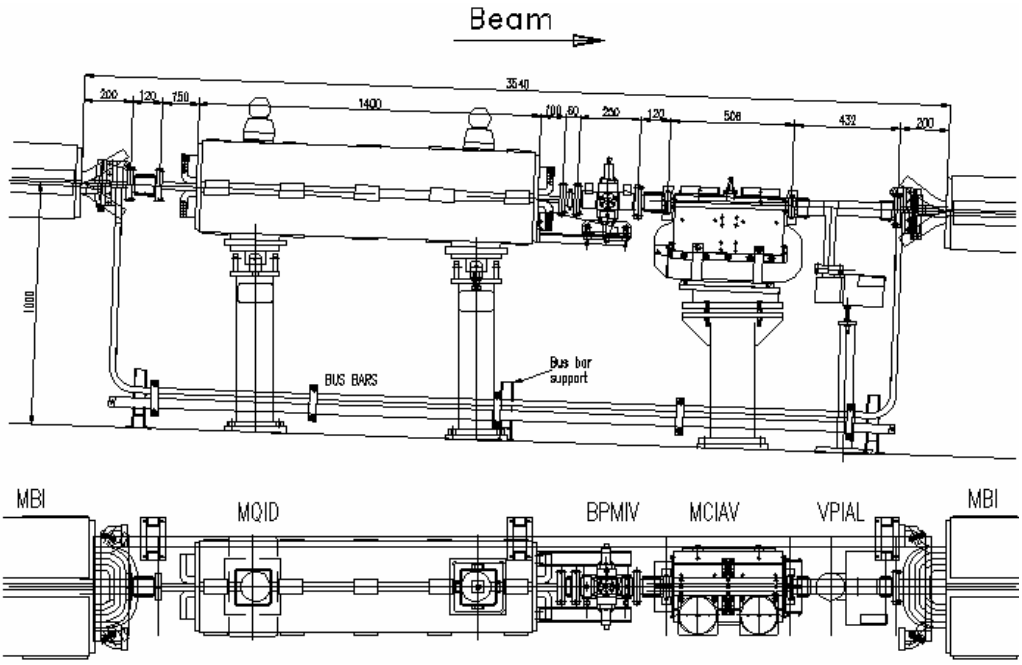

Figure 22.3: Short-straight section layout, showing vertical BPM and corrector.

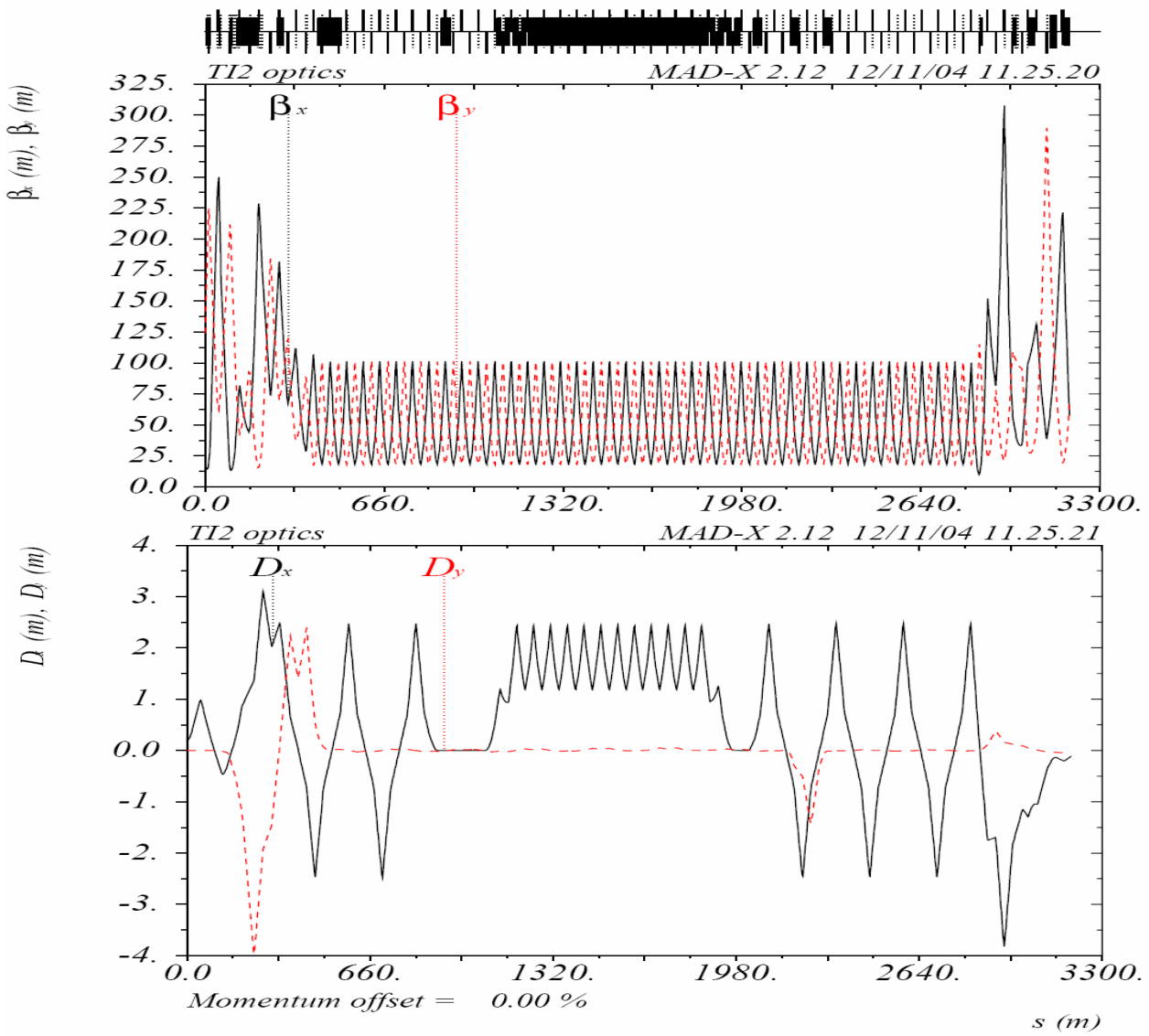

Figure 22.4: TI 2 optics functions.

22.3.1 Optics Design Features and Constraints

The arcs of the transfer lines are matched to the SPS and the LHC by means of sets of dedicated quadrupole magnets on either end of the lines. The six arc constraints in TI 8 are matched to the SPS with seven matching quadrupoles (four quadrupoles in TT40 and three in TI 8). In the case of TI 2 the transfer line arc is matched to the SPS using six quadrupoles in TI 2 (there are also six matching quadrupoles in the existing TT60 line). On the LHC ends, both lines are equipped with 10 matching quadrupoles.

With the present layout the dispersion matching in both planes on the LHC side is difficult and limits the tunability of the lines. This arises from a combination of several issues: the maximum gradient of 57 T/m for the matching quadrupoles, the aperture constraint of $\geq 6\sigma$ in the arc and the aperture bottleneck towards the end of the lines. The additional constraints imposed by the phase advance relations between the transfer line collimators (TCDI) limit the flexibility further. To guarantee sufficient protection, the phase advance conditions between the TCDI must be constrained to within a few degrees of their nominal values. The TCDI system is based on 3-phase collimation (3 collimators per plane with 60° between two subsequent collimators, or 60°+n×180° in case of space problems) and is installed to protect the MSI septum and the LHC cold aperture. The TCDI are located as close as possible to the MSI and the LHC and hence are located in the LHC end matching section. Any changes of the LHC optics at the injection points affect the phase advances in the matching sections, resulting in a trade-off between mismatch to the LHC and protection level

of the TCDI. The optics versions of both lines need to be matched to the LHC optics (presently version v6.5) with the constraints of the layout and powering, to guarantee enough line aperture and the optimum phase advance conditions between the TCDI collimators.

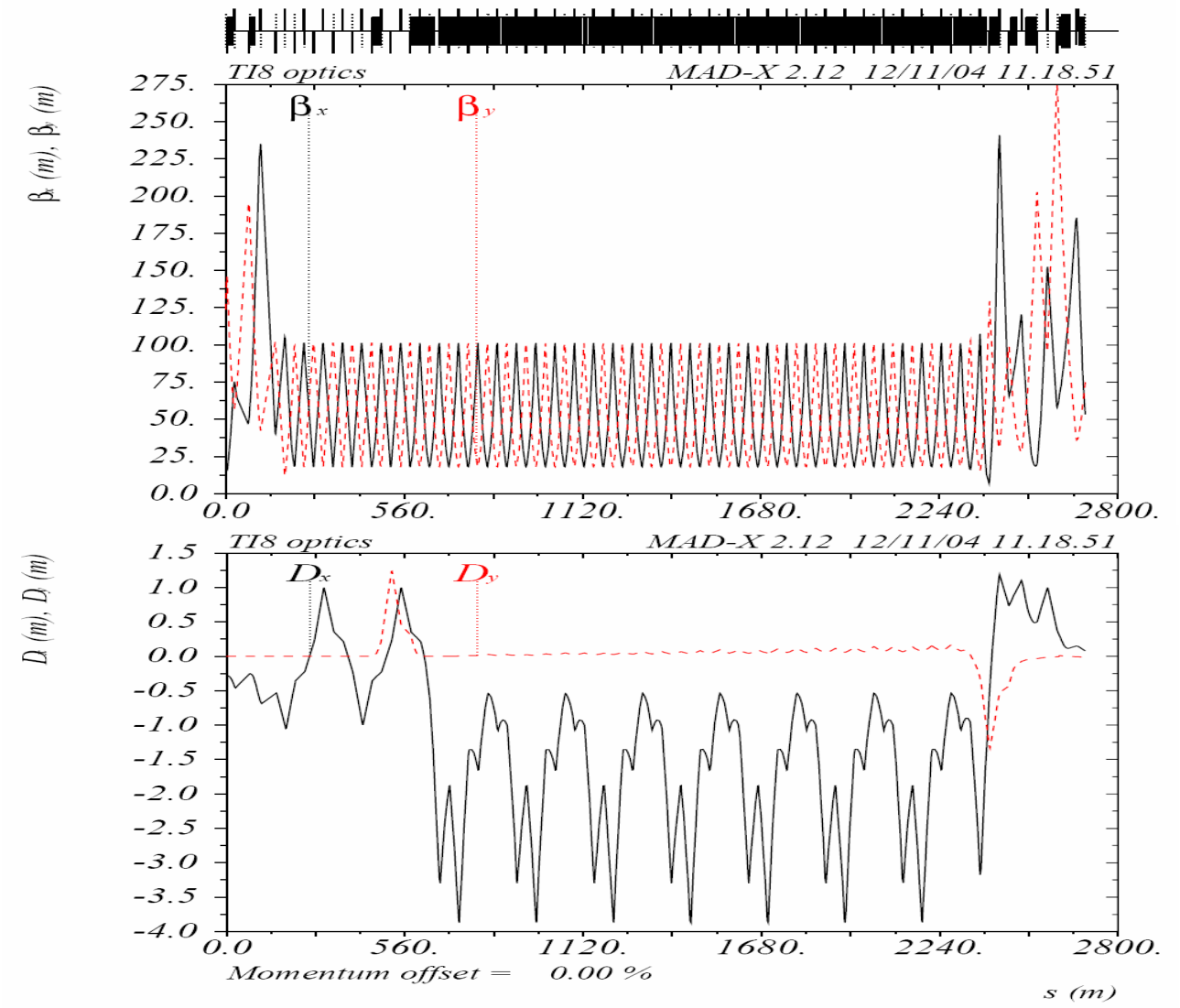

Figure 22.5: TI 8 optics functions.

22.3.2 Mismatch and Errors

The tight emittance budget for transfer and injection into the LHC places stringent requirements on the various mismatch factors which can occur [8]. Mismatch leading to emittance growth can arise from several sources. The total contribution of all of the above effects must be less than the emittance growth budget of 1.07, which presents a difficult challenge. For the effects identified below, this means that each contribution must be below about the 1-2 % level.

Steering error

In the LHC the steering errors are normally dealt with by the damper system and the emittance blow-up will be a function of the injection errors, the damper strength and the filamentation time. For the transfer lines the maximum injection error is specified as $e_{inj} \leq 1.5\ \sigma$. The residual blow-up after the action of the feedback depends on the filamentation and damping times [9]. For the specified filamentation and damping times of 68 ms and 5 ms respectively [10], the maximum 1.5 σ injection error gives an emittance increase of about 0.5 %.

Betatron mismatch

The beam will be optically mismatched [11] when the α and β of the injected beam do not match those of the LHC. This may be due to optical errors in the line, or a mismatch at the SPS extraction point. To respect the emittance budget of about 2% increase, the mismatch parameter λ (defined as the ratio of the largest semi-axes of the mismatched and matched ellipses) must be less than 1.10.

Dispersion mismatch

The dispersion can also be mismatched at the injection point, leading to emittance growth [12]. For an energy spread of about 10^{-3}, the maximum tolerable dispersion mismatch is very small, at about 0.05 m and 0.002 rad, for ΔD and $\Delta D'$ respectively.

Energy error

An energy error between the machines can also lead to an emittance growth. For a nominal dispersion of about 0.1 m, a (relatively pessimistic) energy error of 5×10^{-4} gives an emittance growth of about 0.3 %.

Geometrical mismatch

There can also be a geometrical mismatch at injection with a tilt between the beam XZ plane delivered by the transfer lines and that of the LHC. The expected emittance increase is about 1.3 % given the design tilt mismatch of 52 mrad between TI 8 and the LHC [13].

Coupling

Coupling between the planes in the transfer line can also lead to an emittance growth at injection. For the LHC transfer lines the coupling, **k**, is expected to be less than 5 %. The emittance growth from this source will therefore be below 0.1 %.

Summary

The expected maximum levels of each contribution are given in Tab. 22.4 together with the limits placed on the various optical parameters. The total expected emittance increase is of the order of 6%, which is just inside the specified emittance budget.

Table 22.4: Summary of emittance increase contributions and associated limits on optical parameters.

Effect	**Parameter**	**Unit**	**Limit**	**expected $\varepsilon/\varepsilon_0$**
Steering error	τ_{DC} / τ_d (damping ratio)	-	$\geq$14	
	e_{inj}	σ	$\leq$1.5	1.005
Betatron mismatch	λ (mismatch factor)	-	$\leq$1.1	1.020
Dispersion mismatch	ΔD (dispersion error)	m	$\leq$0.05	
	$\Delta D'$ (dispersion prime error)	rad	$\leq$0.002	1.020
Energy error	$\Delta p/p$	-	$\leq 5\ 10^{-4}$	1.003
Geometrical mismatch	θ (tilt mismatch)	rad	$\leq$0.052	1.013
Coupling	**k** (coupling factor)	-	$\leq$0.05	1.001
Total				**1.063**

22.3.2 Energy Acceptance

The energy acceptance of the line is a function of the aperture, the optics and the corrected trajectory. The specified acceptance in $\Delta p/p$ is $\pm$0.003. For TI 8 the acceptance has been checked by simulating the transmission of a beam as a function of the energy offset, using the full aperture model and the various errors, for 1000 corrected trajectories simulated with all errors. The simulated distribution of transmissions is shown in Fig. 22.6. Defining the acceptance as the 99% transmission limit, the simulation gives an energy acceptance for TI 8 of around $\pm$0.003.

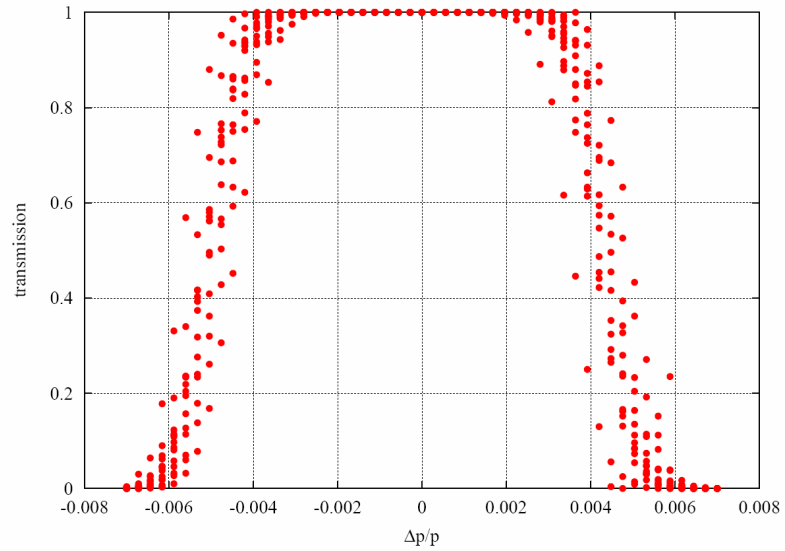

Figure 22.6. Simulated transmission as a function of beam energy offset, for TI 8 with all errors.

22.3.3 Beam tilt accumulation

A horizontal bending dipole aligned with an inclination (slope) angle ϕ with respect to the reference coordinate system introduces a small tilt (roll) angle ψ into the beam. For small angles ψ is proportional to the product of the magnet bending angle α and the slope ϕ. For most transfer lines this effect can be neglected, but for long lines with many horizontal bending magnets on relatively steep vertical slopes relative to the reference frame, a non-negligible tilt angle ψ can accumulate between the local beam plane and the reference alignment system. This can result in a mismatch at injection with subsequent emittance blow-up. In addition other undesirable effects, such as non-orthogonal trajectory measurement and correction can become important. A detailed description of this effect is given in [14].

In TI 8, this effect is significant. The roll angle ψ accumulates along the line, reaching 65 mrad at the LHC injection point. This is much larger than the 13 mrad local tilt of the LHC machine. With no additional measures, the (x,y) plane of the beam would therefore have an inclination of about 52 mrad to that of the beam in the LHC.

There are two separate issues which have to be considered:

Firstly, the accumulation of ψ along the transfer line due to the combination of vertical and horizontal bends. This does not depend very much on whether the line is designed so that the dipole magnets are aligned with zero tilt or with the local beam tilt. However, the quadrupoles, correctors and pickups will be aligned with respect to the local beam tilt to ensure that the system stays orthogonal to simplify the trajectory correction and to avoid coupling between the planes. For TI 8 this means an alignment of up to 3.7° with respect to the vertical of the local CERN reference system.

Secondly, the effect of the mismatch in ψ between the end of the transfer line and the LHC. For the TI 8 injection point this effect is about 52 mrad. Correction can only be accomplished by rotating the plane of the beam with a system of skew quadrupoles at the end of each line. However, the emittance increase expected from this effect is small, below 2 % [12]. A potentially more important effect is the repopulation of the transverse tails of the beam, which are removed above about 3.5 σ in the SPS. Analysis has shown that the coupling between the planes induced by the tilt can populate the beam tail significantly [14], with amplitude growths of around 20%. An effective remedy is to remove particles in the tails which have simultaneous large horizontal and vertical amplitudes by means of a tilted X-Y scraper in the SPS [15]. In this case, skew correction of the tilt plane is not required, since the amplitude growth is less than 10%.

22.4 TRAJECTORY CORRECTION

Following in-depth study [2,16] a correction scheme is used in which two out of every four adjacent cells in each plane are equipped with correctors. Full correction is performed at the beginning and the end of each line. TI 2 uses 55 correctors, while TI 8 requires 43, in addition there are 55 and 46 beam position monitors in the two lines, respectively. The placement of these is designed to keep the maximum trajectory excursion amplitude to below 4.5 mm. Fig. 22.7 shows the distribution of expected maximum trajectory excursions for TI 8.

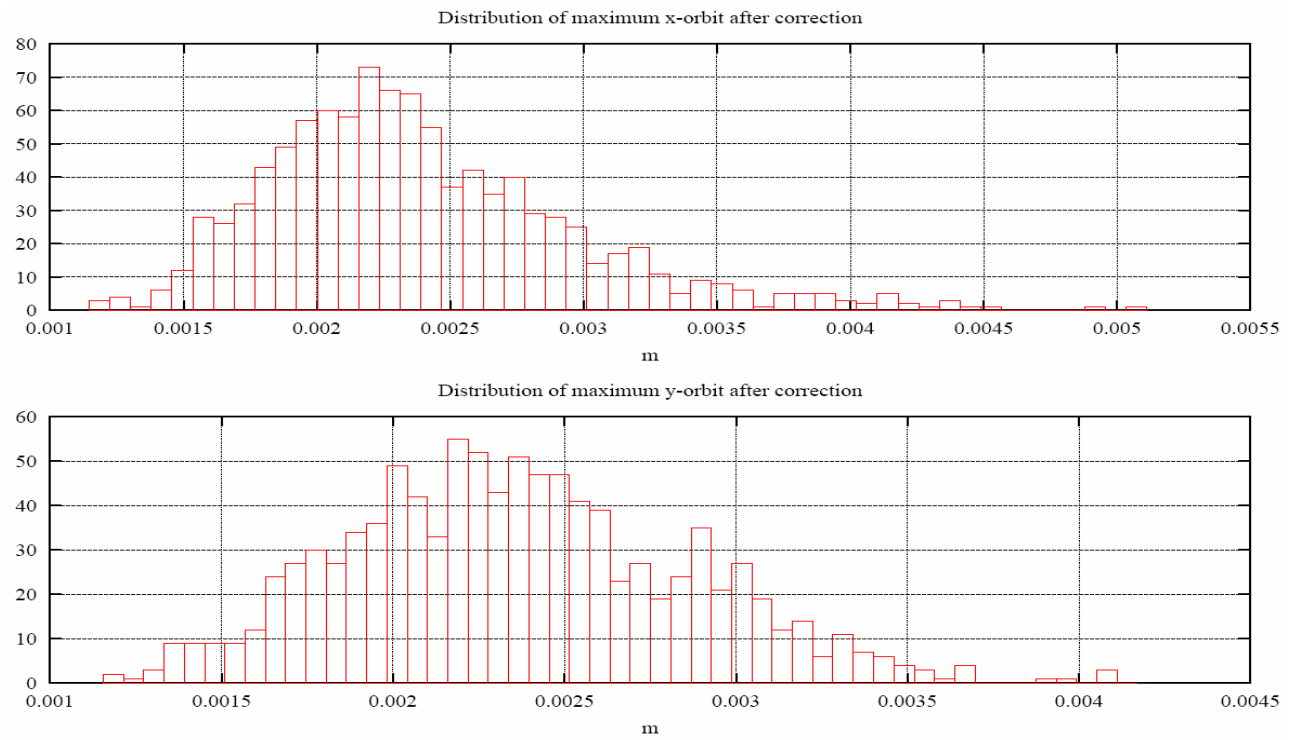

Figure 22.7: Distribution of maximum amplitudes for TI 8, based on 1000 trajectory corrections simulated with all errors.

The study shows that the correctors, including dipole groups, can correct orbit excursion caused by error distributions up to 3σ. Exceptions are found in the correctors in both planes responsible for compensating injection errors, assumed to be Gaussian-distributed with rms equal to 0.5 mm in position and 50 μrad in angle. This deficit in corrector range becomes less severe and eventually vanishes, as the injection error magnitudes are reduced. Fig. 22.8 shows the distribution of expected maximum corrector strengths for TI 8.

For 1-to-1 steering, a missing monitor can lead to a singular steering configuration. This in turn can result in an excessive correction if not handled correctly. In such cases disabling one corrector resolves the problem. In the over-constrained case of the steering in the periodic sections, the configurations are generally less susceptible to excessive corrections as a result of missing monitors.

The limited correcting power for fighting injection errors causes some sensitivity of the trajectory error to the correction process at the beginning of the TI 2 and TI 8 lines. Large peaks are associated with corrector scaling errors, all caused by the same correctors responsible for fixing injection errors. This sensitivity can only be fixed by orbit control upstream of the injection point.

The difficulties which might arise with monitor anomalies illustrate the importance of an intelligent trajectory correction algorithm. The best way to deal with a missing monitor is not always to disable individual correctors, but to disable singular combinations of correctors, achievable only through the use of an intelligent real-time algorithm.

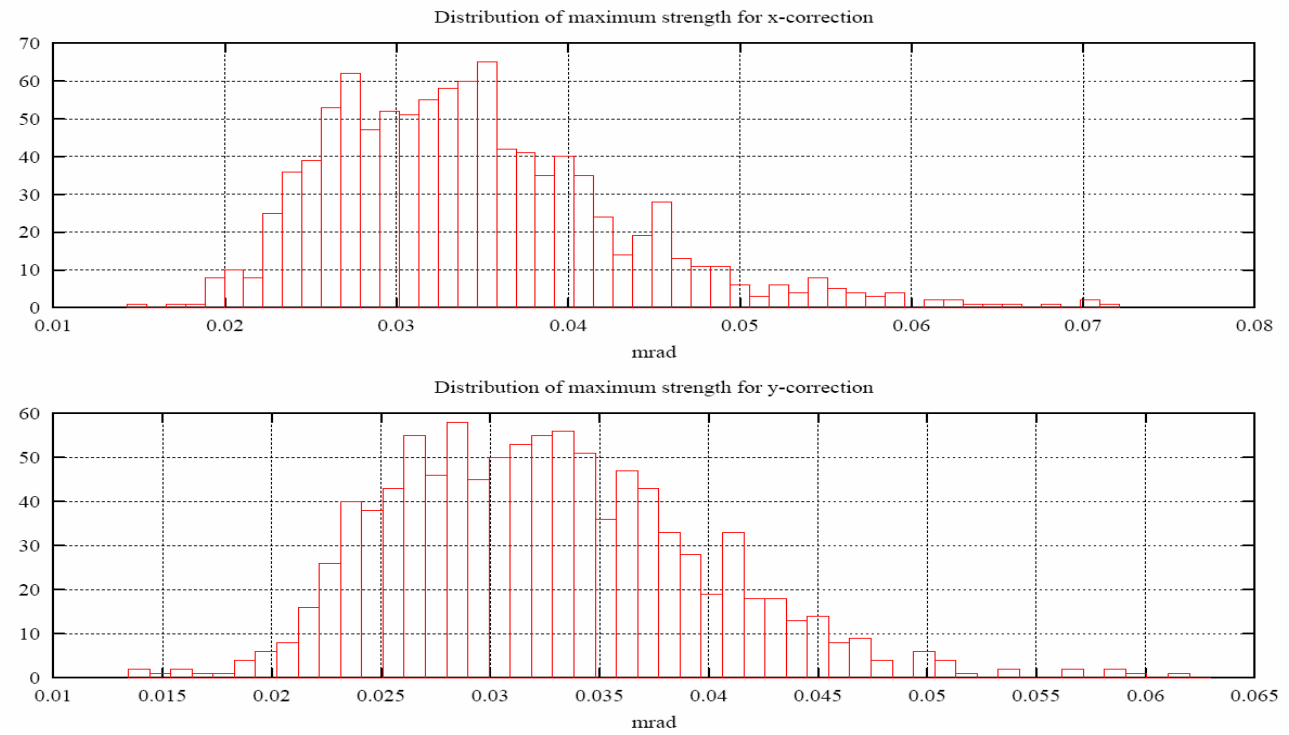

Figure 22.8: Distribution of maximum corrector strengths for TI 8, based on 1000 trajectory corrections simulated with all errors.

22.4.1 Tolerances

Full errors were included in the calculation of the trajectory, for the correction studies and for the aperture calculations. The values used are shown in Table 22.5.

Table 22.5: Tolerances assumed in the trajectory correction studies.

Error	**Distribution**	**Unit**	**width**	**truncation**
Main quadrupole lateral alignment	Gaussian	mm	0.2 (1 σ)	±3 σ
Main quadrupole tilt	Gaussian	mrad	0.2 (1 σ)	±4 σ
Main dipole (MBI) field	Gaussian	$\Delta B/B_{nom}$	2.5×10^{-4} (1 σ)	±2 σ
Main dipole tilt	Gaussian	mrad	0.2 (1 σ)	±4 σ
BPM position / electrical	Flat	mm	0.5 (full width)	
Injection position	Gaussian	mm	0.1 (1 σ)	±3 σ
Injection angle	Gaussian	mrad	0.001 (1 σ)	±3 σ
Power supply ripple (MBI)	Gaussian	$\Delta I/I_{nom}$	2.5×10^{-5}	±2 σ
Power supply ripple (other families)	Gaussian	$\Delta I/I_{nom}$	5.0×10^{-5}	±2 σ

22.5 BEAM STABILITY AT INJECTION INTO THE LHC

The beam transferred into the LHC may have position and angle offsets with respect to the nominal orbit. These offsets will have an impact on several aspects of the injection process. The effects which contribute to the errors at the LHC injection point include the performance of the elements in the SPS extraction channels, the SPS to LHC transfer lines and the LHC injection systems themselves. The overall performance of the beam transfer system has been analysed [5] for random and systematic effects, in terms of the expected delivery precision of the injected beam. For both transfer lines the rms variation at the injection point coming

from the random effects in various elements is about 0.35 σ horizontally and 0.30 σ vertically. For these effects the whole beam will be injected at the specified amplitude, since the period of the power converter ripple (~milliseconds) is much longer than the batch length (~10 μs). A further systematic offset of about ±0.25 σ horizontally and ±0.35 σ vertically has to be added for the kicker waveform. The variation along the kicker pulse will reproducibly sweep the bunches in each batch over this range. The bunches are not uniformly distributed within this range and the resulting oscillations have implications for the performance of the damper. This is especially true in the vertical plane as a result of the high frequency components present in the early part of the MKI pulse. Taking a 99% (3 σ) confidence limit for the random effects, the overall precision is then 1.25 σ in both H and V for LHC beams 1 and 2. This is within the specification of 1.5 σ. The distribution of the bunches in the vertical plane will have implications for the setting-up of the injection into the LHC, since normally one would try to inject the average bunch position onto the LHC orbit. If this is done with the bunch distribution from the MKI, the actual range of offsets coming from the MKI waveform will be +0.2 to -0.5 σ. The random effect in the vertical plane is dominated by the precision of the SPS orbit and any drifts in the transfer line. In the horizontal plane the contributions from the orbit, drift and main magnet families are of a similar order of magnitude.

22.6 APERTURE

The transferred beams must stay within the available aperture. The strongest aperture constraint comes from the main dipoles of the transfer line, the MBI, with their full gap height of only 25 mm. This aperture results in a maximum tolerable vertical trajectory excursion, near the defocusing quadrupoles, of ±4.5 mm.

The aperture N in number of sigma available to the beam is derived using:

$$N = ([A/2 - E_{\max}(\beta/\beta_{\max})^{1/2} - K_{\beta}D.\Delta p/p]/K_{\beta})/\sigma$$

here, A is the full physical aperture remaining after mechanical and alignment tolerances and sagitta are taken into account. K_β = 1.1 is the optical mismatch parameter, β_{max} the maximum beta function in the regular arc, E_{max} the maximum allowed orbit excursion, $\sigma = (\beta\,\varepsilon)^{1/2}$ the betatron beam size and $\Delta p/p = 0.0015$ the momentum spread.

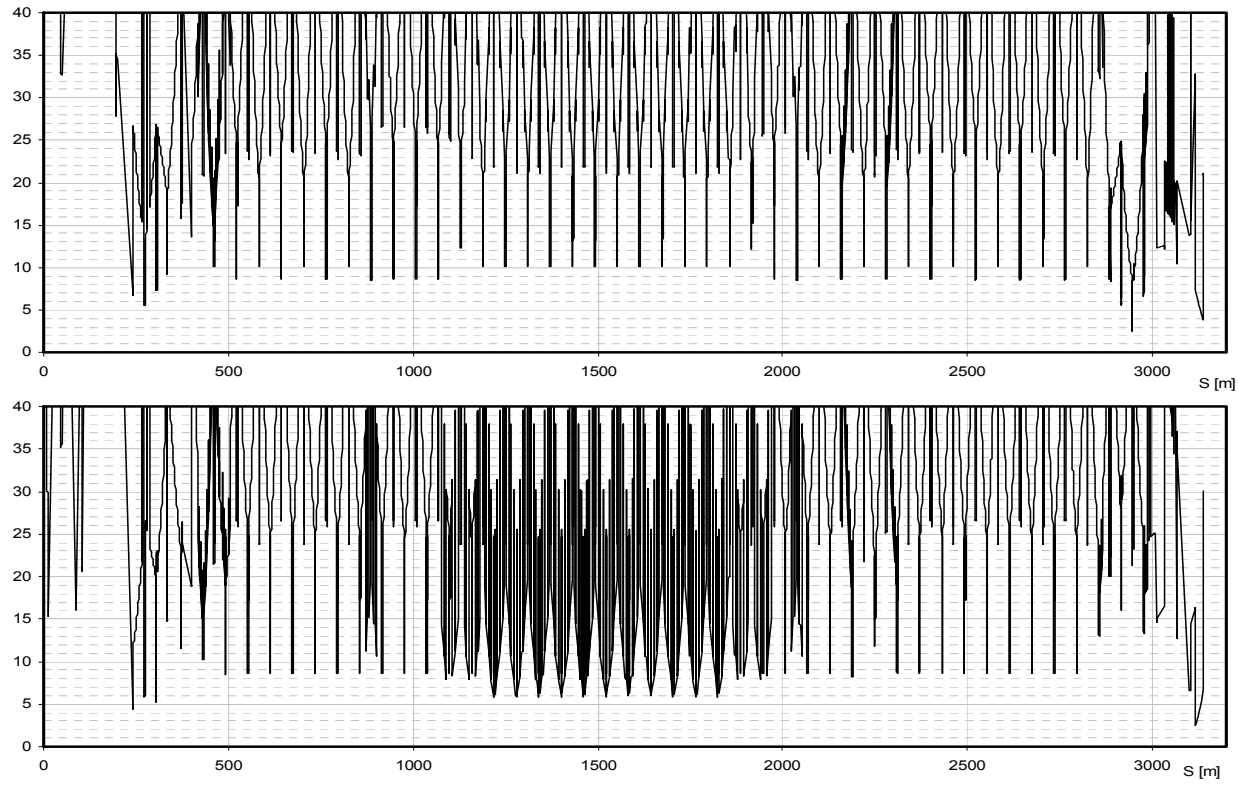

Figure 22.9: Horizontal (top) and vertical beam aperture (σ) for TI 2.

Figs. 22.9 and 22.10 show the aperture N calculated for the horizontal and vertical planes of the two lines, using the full physical aperture model. Fig. 22.11 shows the distribution of apertures expected at the six worst aperture bottlenecks in TI 8. This was based on the result of 1000 corrected trajectories simulated with all errors.

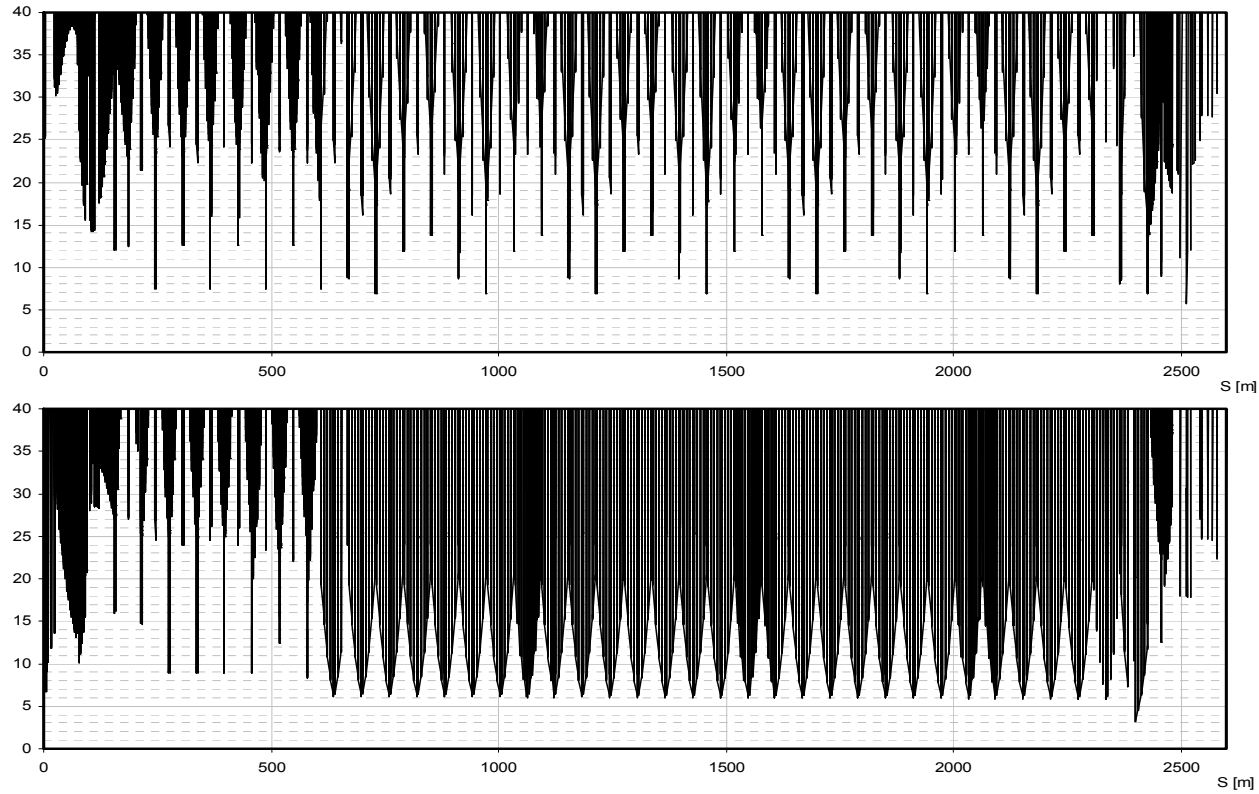

Figure 22.10: Horizontal (top) and vertical beam aperture (s) for TI 8.

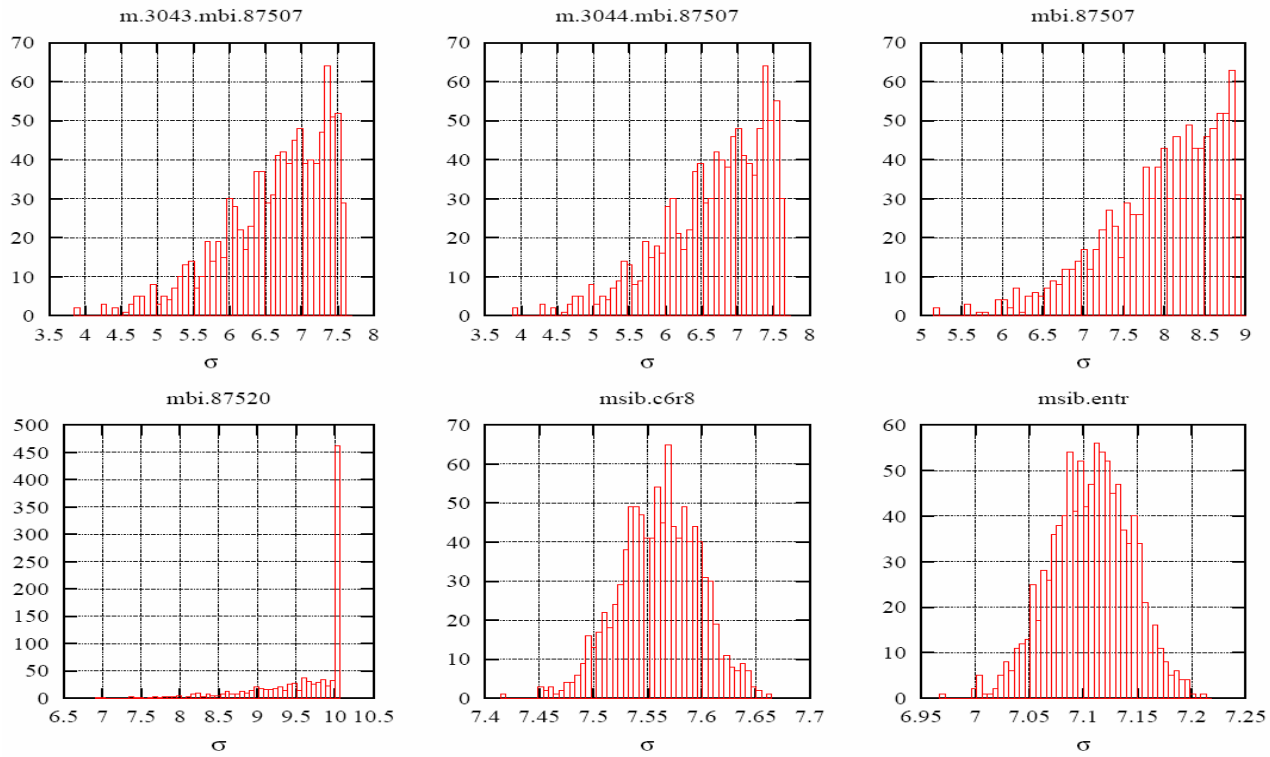

Figure 22.11: Aperture bottlenecks in TI 8. Histograms show the simulated aperture remaining for the beam for 1000 corrected trajectories, after all errors are included.

22.7 INTERLOCKS AND SURVEILLANCE

The beam parameters mean that the bunches must stay within the available aperture to avoid severe damage to components. For some of the power supplies this corresponds to an error of just 10^{-3}, which is assumed to be the interlock level for the power supply current surveillance. The power supplies must be surveyed until the last few milliseconds before extraction, to minimise the risk of a trip and a disastrous reduction in the current.

The interlocking of the SPS extractions and LHC injections are intimately linked to the transfer line interlocks and must ensure that out-of-tolerance beams cannot be extracted, transferred or injected. The use of passive protection devices is already widespread, with the TPSG in the extraction channel, the TCDI collimators in the transfer line and the TDI, TCDD and TCLI collimators in the injection regions of the LHC.

REFERENCES

[1] A. Hilaire et al., "*Beam Transfer to and Injection into LHC*", EPAC'98, Stockholm, June 1998 and CERN/LHC Project Report 208.

[2] A. Hilaire et al., "*Trajectory Correction of the LHC Injection Transfer Lines TI 2 and TI 8*", CERN/LHC Project Report 122.

[3] A.Hilaire et al., "*The Magnet System of the LHC Injection Transfer Lines TI 2 and TI 8*", LHC-Project-Note-128; CERN, 1998.

[4] O. Brüning, J. B. Jeanneret, "*Optics Constraints Imposed by the Injection in IP2 and IP8*", CERN/LHC Project Note 141 (1998).

[5] B.Goddard, "*Expected delivery precision of the injected LHC beam*", CERN/LHC Project note 337, 2004.

[6] J.Borburgh et al., "*The Design of the New Fast Extraction Channel for the LHC*", EPAC'04, Lucerne 2004. CERN-LHC-Project-Report-752, CERN, 2004.

[7] B. Goddard et al., "*The new Extraction Channel for LHC and CNGS*", EPAC'00, Vienna, 2000, CERN SL 2000-036 (BT), 2000.

[8] B.Goddard, V.Kain, "*Expected emittance growth from errors at injection into the LHC*", to be presented at PAC'05, Tennessee 2005.

[8] L.Vos, "*Transverse emittance blow-up from dipole errors in proton machines*", LHC-Project-Report-193, CERN, 1998.

[9] W.Hofle et al., "*Transverse damping system for the future CERN LHC*", PAC 2001.

[10] P.M.Hanney and E.Keil, "*How does betatron mismatching affect beam size and density?*", CERN-ISR-TH/69-32, 1969.

[11] G.Arduini, P.Raimondi, "*Transverse emittance blow-up due to injection errors*", SL-Note-99-022-SLI, CERN, 1999.

[12] T.Risselada, "*Evaluation of the emittance blow-up at injection due to beam tilt in the LHC injection lines*", CERN Beam Physics Note 76, 2004.

[13] B.Goddard et al., "*Geometrical alignment and associated beam optics issues of transfer lines with horizontal and vertical deflection*", LHC-Project-Report-719; CERN, 2004.

[14] V.Kain, *Notes of the LHC Injection Working Group Meeting held on meeting held on 28 July 2004*

[15] H.Burkhardt, R.Schmidt, "*Intensity and Luminosity after Beam Scraping*", CERN-AB-2004-032-ABP; CERN, 2004.

[16] Y.Chao & V.Mertens, "*Analysis and Optimisation of Orbit Correction Configurations Using Generalised Response Matrices and its Application to the LHC Injection Transfer Lines TI 2 and TI 8*", LHC-Project-Report-470; CERN, 2001.